Analysis of the conformation of the 3' major domain of Escherichia coli16S ribosomal RNA using site-directed photoaffinity crosslinking

A. Montpetit, C. Payant, J. M. Nolan and L. Brakier-Gingras

RNA 1998 4: 1455-1466

RNA (1998), *4*:1455–1466. Cambridge University Press. Printed in the USA.

Analysis of the conformation of the 3′ major domain of *Escherichia coli* 16S ribosomal RNA using site-directed photoaffinity crosslinking

ALEXANDRE MONTPETIT,[1] CATHERINE PAYANT,[1] JAMES M. NOLAN,[2] and LÉA BRAKIER-GINGRAS[1]

[1]Département de Biochimie, Université de Montréal, Montréal, Québec H3T 1J4, Canada
[2]Department of Biochemistry, Tulane University Medical Center, New Orleans, Louisiana 70112, USA

ABSTRACT

The 3′ major domain of *Escherichia coli* 16S rRNA, which occupies the head of the small ribosomal subunit, is involved in several functions of the ribosome. We have used a site-specific crosslinking procedure to gain further insights into the higher-order structure of this domain. Circularly permuted RNAs were used to introduce an azidophenacyl group at specific positions within the 3′ major domain. Crosslinks were generated in a high-ionic strength buffer that has been used for ribosome reconstitution studies and so enables the RNA to adopt a structure recognized by ribosomal proteins. The crosslinking sites were identified by primer extension and confirmed by assessing the mobility of the crosslinked RNA lariats in denaturing polyacrylamide gels. Eight crosslinks were characterized. Among them, one crosslink demonstrates that helix 28 is proximal to the top of helix 34, and two others show that the 1337 region, located in an internal loop at the junction of helices 29, 30, 41, and 42, is proximal to the center of helix 30 and to a segment connecting helix 28 to helix 29. These relationships of vicinity have previously been observed in native 30S subunits, which suggests that the free domain adopts a conformation similar to that within the 30S subunit. Furthermore, crosslinks were obtained in helix 34, which suggest that the upper and lower portions of this helix are in close proximity.

Keywords: 16S ribosomal RNA; photoaffinity crosslinking; RNA structure

INTRODUCTION

Ribosomal RNA plays a major role in protein synthesis, and a detailed knowledge of its structure is required to elucidate the mechanisms underlying its function. However, the size of the large rRNAs has so far precluded the use of nuclear magnetic resonance spectroscopy (NMR) to solve their structure (reviewed in Green & Noller, 1997). Crystals of the entire ribosomes and ribosomal subunits have been obtained, but the crystal structures have not yet been solved at atomic resolution (Thygesen et al., 1996; Ban et al., 1998 and references therein).

A general property of large RNAs is that they can be dissected into smaller domains that conserve the ability to fold correctly. This reductionist approach has recently been applied to analyze the conformation of a variety of RNA domains with NMR or X-ray crystallography. As examples, structures have been determined by NMR for the decoding center of 16S rRNA complexed with an aminoglycoside antibiotic (Fourmy et al., 1996), for two important regions of 23S rRNA (the α-sarcin loop (Szewczak & Moore, 1995) and the 2250 hairpin loop, involved in peptidyl-tRNA binding (Viani-Puglisi et al., 1997)), and for loops D and E of 5S rRNA (Dallas & Moore, 1997). Crystal structures have been determined for the P4–P6 domain of group I intron (Cate et al., 1996), the largest RNA yet crystallized with 160 nt, and for fragment I of 5S rRNA (Correll et al., 1997).

Our goal is to characterize spatial relationships in *Escherichia coli* 16S rRNA. It has been shown that, in vitro, in high-ionic strength reconstitution buffer (20 mM Mg^{2+}, 300 mM K^{+}), each of the three domains that constitute this RNA (5′, central and 3′) can interact with the specific subset of proteins with which they interact when they are part of the intact 16S molecule (Weitzmann et al., 1993; Samaha et al., 1994; Agalarov et al., 1998). This implies that each domain can fold independently of the rest of the molecule.

Reprints requests to: Léa Brakier-Gingras, Département de Biochimie, Université de Montréal, 2900 blvd Edouard-Montpetit, Montréal, Québec H3T 1J4, Canada; e-mail: gingras@bcm.umontreal.ca

We have decided to investigate the conformation of the 3′ major domain of 16S rRNA in ribosome reconstitution buffer, in the absence of ribosomal proteins. The 3′ major domain is involved in several functions of the ribosome (reviewed by Zimmermann, 1996). It interacts with mRNA (Juzumiene et al., 1995; Sergiev et al., 1997), initiation factor IF2 (Wakao et al., 1991), and elongation factor G (Wilson & Noller, 1998). Helix 34, in the upper part of the domain, contains the binding site of the antibiotic spectinomycin, an inhibitor of translocation (Makosky & Dahlberg, 1987; Bilgin et al., 1990; Brink et al., 1994), it interacts with the termination factors (Murgola, 1996; Arkov et al., 1998), and it is involved in subunit association (Herr et al., 1979; Baudin et al., 1989). Furthermore, mutations in helix 34 were found to affect translational accuracy (Moine & Dahlberg, 1994; O'Connor et al., 1997). The lower part of the domain contains nucleotides which are involved in the binding of tRNAs at the P site (Moazed & Noller, 1990; von Ahsen & Noller, 1995; Joseph et al., 1997), and which have been crosslinked to the A-, P- and E-site-bound tRNAs (Döring et al., 1994). Tetracycline, an inhibitor of tRNA binding to the A site, also interacts with this part of the domain (Oehler et al., 1997).

To study the conformation of the large rRNA domains, indirect techniques, such as chemical probing and crosslinking, can provide useful information since NMR and X-ray crystallography are still inadequate. Random crosslinking has been extensively used to study the higher-order structure of rRNAs (Wilms et al., 1997; reviewed in Baranov et al., 1998b). Site-directed crosslinking has been used by the groups of Brimacombe and Cooperman but results are still scarce (Alexander & Cooperman, 1998 and references therein; Baranov et al., 1998a). The technique developed by Brimacombe and his coworkers involves the site-specific fragmentation of 16S rRNA with RNase H and the addition of a photoreactive nucleotide at the 3′ end of the 5′ fragment. Its use is limited by the capacity of the two fragments to be reconstituted into a 30S subunit. The procedure of the Cooperman group involves the hybridization to a specific portion of rRNA within the ribosome of a complementary photolabeled DNA probe. However, this technique requires the rRNA portion that is probed to be exposed and single-stranded, and, moreover, the binding of the probe itself can induce conformational rearrangements. Pace and his coworkers have developed a site-specific crosslinking procedure that was successfully applied to study the conformation of RNase P RNA (Nolan et al., 1993; Harris et al., 1994, 1997). It utilizes circularly permuted RNAs, in which the native 5′ and 3′ extremities are joined by a synthetic oligonucleotide linker and novel 5′ and 3′ extremities are relocated in the interior of the sequence. The novel 5′ termini are modified by coupling to a photoaffinity crosslinking agent, the *p*-azidophenacyl (APA) bromide. This method offers the advantage that it enables us to probe the three-dimensional environment of every G in any RNA molecule. It is imperative, however, to ensure that the discontinuities in the sugar–phosphate backbone that are introduced between the novel 3′ and 5′ ends of the circularly permuted RNAs do not perturb the conformation of the molecule.

In this study, in order to refine our understanding of the higher-order structure of the 3′ major domain, we have utilized the site-directed crosslinking procedure developed by Pace and his coworkers. Seven sites were selected for the introduction of the crosslinking agent: G993, G1047, and G1193 (located in the upper half of the domain, in and around helix 34), and G1309, G1337, G1343, and G1353, in the lower half of the domain. The results presented here will be discussed with respect to their agreement with current models of 16S RNA structure.

RESULTS

Construction and reassembly of circularly permuted RNAs of the 3′ major domain of 16S rRNA

Plasmid pFD33, which contains duplicate copies of the sequence coding for the 3′ major domain of *E. coli* 16S rRNA, was constructed by a three-fragment ligation as described in Materials and Methods and Figure 1. Polymerase chain reaction (PCR) amplification of pFD33 with appropriate primers (see Table 1) resulted in the production of templates coding for the circularly permuted RNAs (cpRNAs) under control of a T7 promoter. In the corresponding transcripts, positions 921 and 1396 of helix 28 are joined by a terminal GCAA tetraloop. Seven new locations for the 5′ endpoint in the RNA were investigated (Fig. 2).

To ascertain that the introduction of discontinuities at different positions within the 3′ major domain did not perturb its conformation, we verified that the different cpRNAs were able to assemble into ribonucleoprotein particles when incubated with a mixture of 30S ribosomal proteins. As mentioned in the Introduction, Samaha et al. (1994) previously showed that the complete 3′ domain, including the major and minor portions, could fold independently of the rest of the RNA molecule and assemble with specific ribosomal proteins into a ribonucleoprotein particle, when incubated with a mixture of 30S ribosomal proteins in reconstitution buffer (20 mM Mg^{2+}, 300 mM K^{+}). We first showed that the native 3′ major domain alone behaved exactly as the complete 3′ domain and interacted with the same subset of proteins (data not shown). We next systematically assessed the capacity of the different cpRNAs to assemble into ribonucleoprotein particles, and found that all the cpRNAs analyzed behaved as the native 3′ major domain, assembling with an efficiency superior

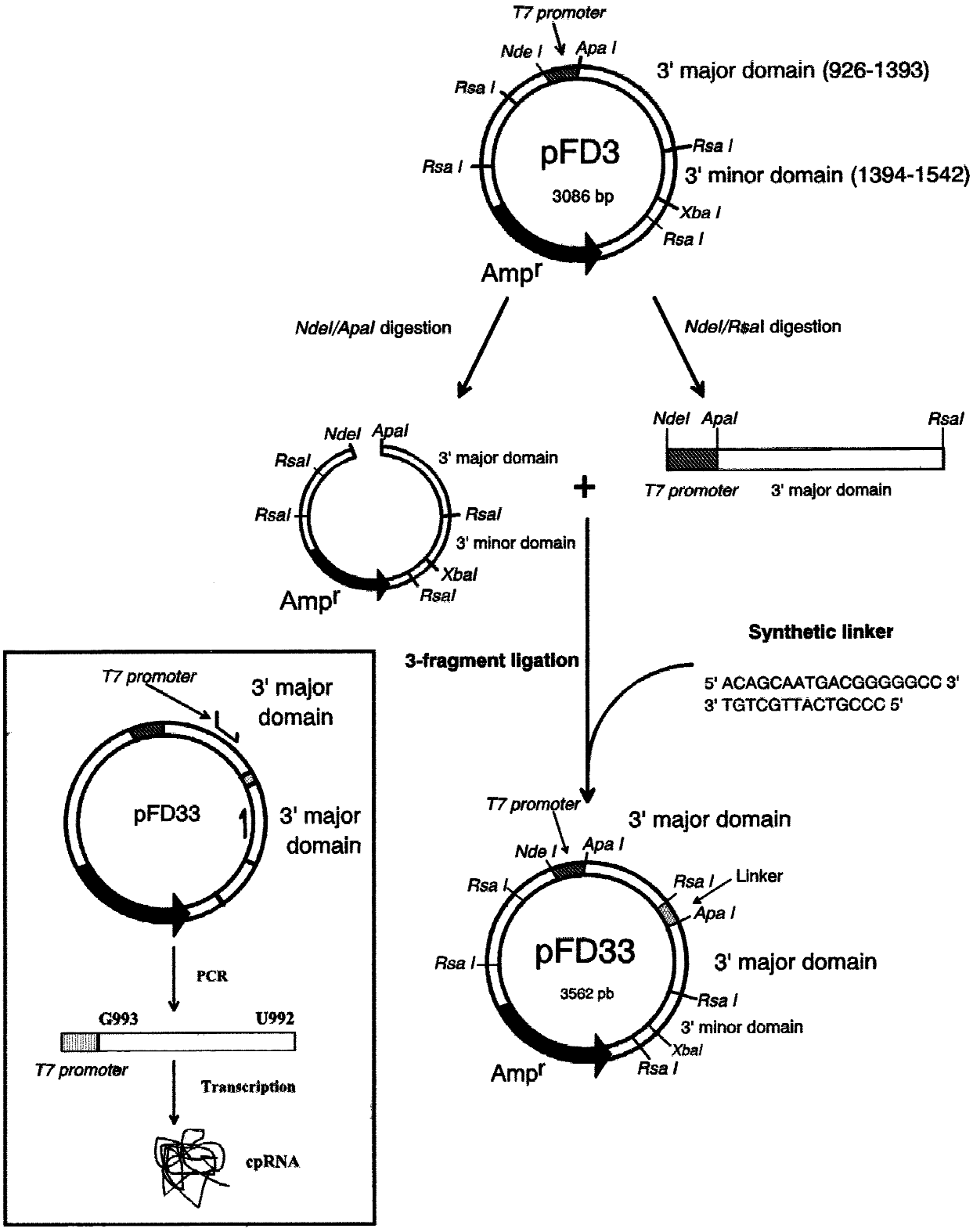

FIGURE 1. Construction of plasmid pFD33. Plasmid pFD33 was generated by a three-fragment ligation (see details in Materials and Methods) and contains two copies of the coding sequence for the 3′ major domain of *E.coli* 16S rRNA. This plasmid was used as a template for PCR amplification of various circularly permuted derivatives of the 3′ major domain coding sequence. The inset illustrates the production of a template that generates a cpRNA by in vitro transcription. ↘ and ← represent the forward primer with a T7 promoter and the reverse primer, respectively.

TABLE 1. Primers used for constructing cpRNA templates.

Name of the permutation		Sequence of the primer[a]
cp993	forward	5′ **TAATACGACTCACTATA**GACATCCACGGAAGTTTTC 3′
	reverse	5′ AAGACCAGGTAAGGTTC 3′
cp1047	forward	5′ **TAATACGACTCACTATA**GGTGCTGCATGGCTGTCGT 3′
	reverse	5′ TGTCTCACGGTTCCCGA 3′
cp1193	forward	5′ **TAATACGACTCACTATA**GTCAAGTCATCATGGCC 3′
	reverse	5′ GTCATCCCCACCTTCCT 3′
cp1309	forward	5′ **TAATACGACTCACTATA**GGAGTCTGCAACTCGACTC 3′
	reverse	5′ AATCCGGACTACGACGCACT 3′
cp1337	forward	5′ **TAATACGACTCACTATA**GGAATCGCTAGTAATCGTG 3′
	reverse	5′ GACTTCATGGAGTCGAG 3′
cp1343	forward	5′ **TAATACGACTCACTATA**GCTAGTAATCGTGGATCA 3′
	reverse	5′ GATTCCGACTTCATGGA 3′
cp1353	forward	5′ **TAATACGACTCACTATA**GTGGATCAGAATGCCAC 3′
	reverse	5′ GATTACTAGCGATTCCGA 3′

[a]The promoter sequence for phage T7 RNA polymerase is shown in bold.

to 90% into a particle that comigrated with the particle generated by the native 3′ major domain in a 5–20% sucrose gradient (Fig. 3). This shows that these cpRNAs fold into the conformation recognized by the ribosomal proteins, indicating that the structure of the domain is not affected by the presence of the novel 5′ and 3′ ends created in each cpRNA.

Crosslinking of the cpRNAs

Transcription with T7 polymerase of the PCR products in the presence of guanosine monophosphorothioate (GMPS) yielded RNAs with a unique sulfur atom at their 5′ end. This sulfur was conjugated to the photoactivable agent, APA bromide. The 5′-APA-cpRNAs were renatured at 43 °C in reconstitution buffer and exposed to UV light (310 mm) for 15 min. Under these conditions, the azido group of APA is converted into a highly reactive nitrene compound, which can form a large variety of covalent bonds within a 10 Å radius.

Figure 4A illustrates the fractionation of crosslinked species with cp1337. Three crosslinked species were found after UV irradiation of APA-coupled transcripts (Fig. 4A, bands a, b, and c, lanes 4 and 5). An additional band (α) also appeared in the absence of APA and independently of UV irradiation, but disappeared in the presence of dithiothreitol (DTT) (Fig. 4A, lanes 2–5), which indicates that this band corresponds to a dimer resulting from formation of a disulfide bond between GMPS-initiated RNAs. No crosslinked species was seen with RNA generated by transcription in the absence of GMPS (Fig. 4A, lane 1). To confirm that only intramolecular crosslinks were obtained apart from band α, we verified that dilution of the RNA (up to 100-fold) did not affect the crosslinking pattern (data not shown). Only crosslinked species that were found consistently in every experiment were chosen for detailed analysis. In the absence of Mg^{2+} and K^+ ions, bands cp1337 a and b disappeared, strongly suggesting that they correspond to tertiary proximities in contrast to band c, which is observed independently of the ionic strength (Fig. 4A, lane 6). Every cpRNA was investigated as described for cp1337. Figure 4B shows the pattern of crosslinking in reconstitution buffer for cp993, cp1047 and cp1193. The dependence of the crosslinked species on the presence of Mg^{2+} and K^+ ions is examined below (see Table 2).

Analysis of crosslinked species

Primer extension by reverse transcriptase was used to map the crosslink sites from gel-purified RNA. Comparison of extension products with sequencing reactions identified the crosslinked nucleotides. For each crosslinked species, the entire sequence was investigated. Examples of this analysis are shown in Figure 5 for crosslinked species derived from cp993, cp1047 and cp1193. Crosslinked nucleotides are visible as primer extension stops. To confirm the primer extension analysis, we examined the mobility of the crosslinked species in denaturing polyacrylamide gels relative to the mobility of the linear molecules (Harris et al., 1997). We found that the relative rate of migration of each of the crosslinked species correlated with the assignment of crosslink sites, as long as the size of the crosslinked loops was less than 80% of the size of the full-length domain (Fig. 6). It is known that the reverse transcriptase may be able to read through some of the crosslinked nucleotides (Burgin & Pace, 1990), which occurred for band a from cp1193. In this case, the size of the crosslinked loop could be used to identify the crosslinked region.

Table 2 summarizes our results. Except for circular forms, where the 5′ and 3′ ends are crosslinked together, no specific crosslink was observed with the native 3′ major domain and with constructions cp1309,

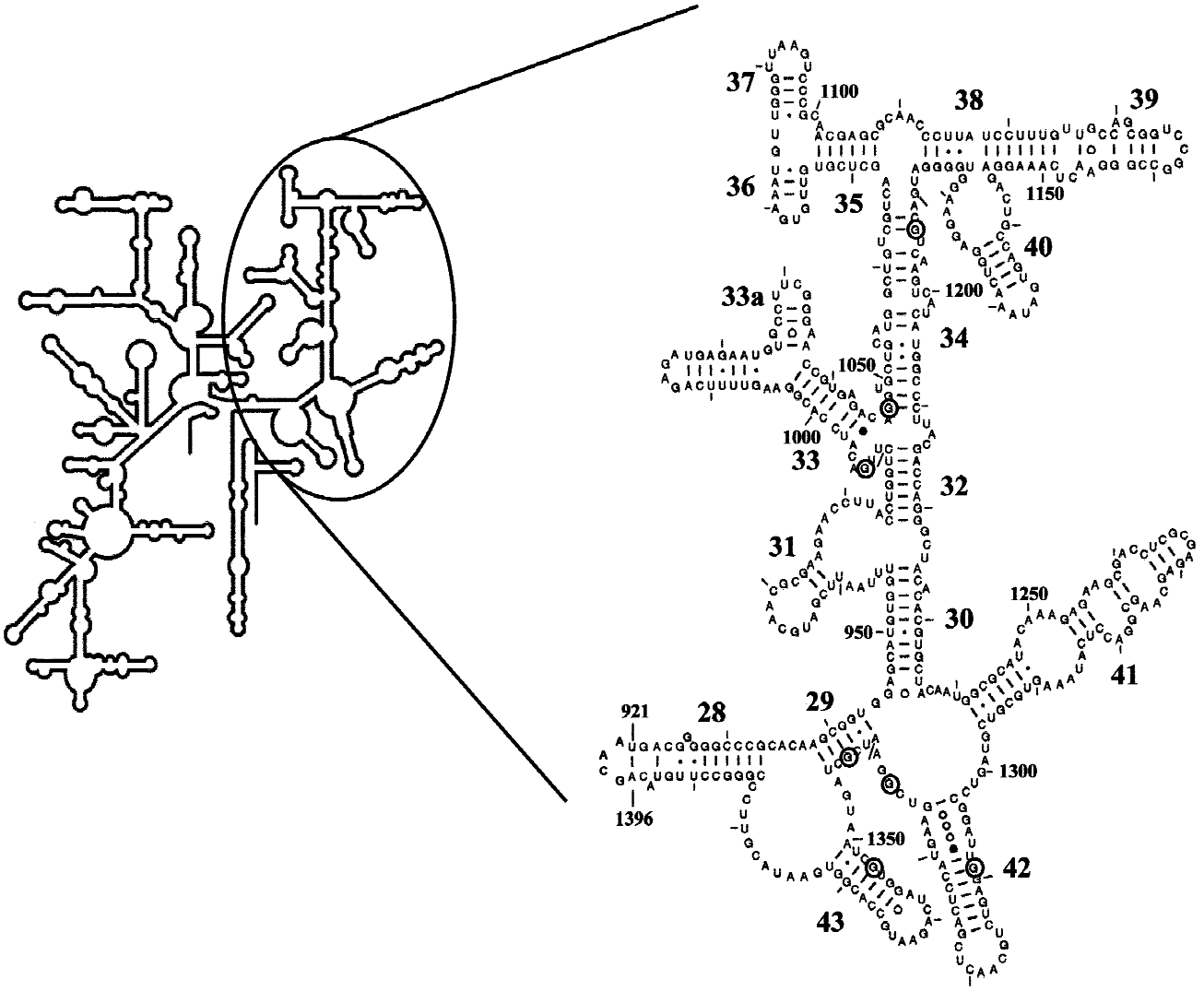

FIGURE 2. Locations of photoagent attachment sites. The skeleton of 16S rRNA secondary structure is presented with an enlarged area corresponding to the 3′ major domain. The photoagent attachment sites located at the 5′ end of each permutation are circled. Nucleotides are numbered as in the 16S rRNA and helices are numbered according to the nomenclature of Brimacombe (1991). The terminal GCAA tetraloop has been introduced to close helix 28.

cp1343 and cp1353. In these molecules, the photoagent probably occupies a position that favors a reaction with the solvent. Eight intramolecular crosslinks were observed with the other positions investigated. The circular forms were observed independently of the presence or absence of Mg^{2+} and K^+ ions, whereas except for crosslinks II and VI, which connect the opposite strands of a helix (see Fig. 7), all the other crosslinks disappeared in the absence of Mg^{2+} and K^+ ions. This demonstrates that, for these crosslinks to occur, the domain must have a specific conformation. The efficiencies of the crosslinks varied from about 1 to 10%. These efficiencies may reflect the distance between the crosslink sites and the 5′ terminus bearing the crosslinking agent (the maximum span covered by the agent being about 10 Å), the relative reactivity of the crosslinking agent with the chemical groups in its vicinity, and the orientation of the modified phosphate relative to its target.

Figure 7 presents our results in the secondary structure of the 3′ major domain. It can be seen that G1193, in the upper stem of helix 34, crosslinked to a bulge at the base of helix 33 (crosslink V), and this crosslink therefore indicates that the upper stem of helix 34 is proximal to its lower stem. G1193 also crosslinked to the region around 1060 (crosslink VI), on the opposite strand, and to region 1395 in helix 28, the helix that connects the head of the 30S subunit to its body (crosslink IV). G993, in the bulge flanking the base of helix 33, crosslinked to a segment spanning the lower half of helix 34 plus the upper stem of this helix (crosslink I), supporting the observation with crosslink V that the upper and lower stems of helix 34 are in close proximity. G1047 crosslinked to the same segment spanning

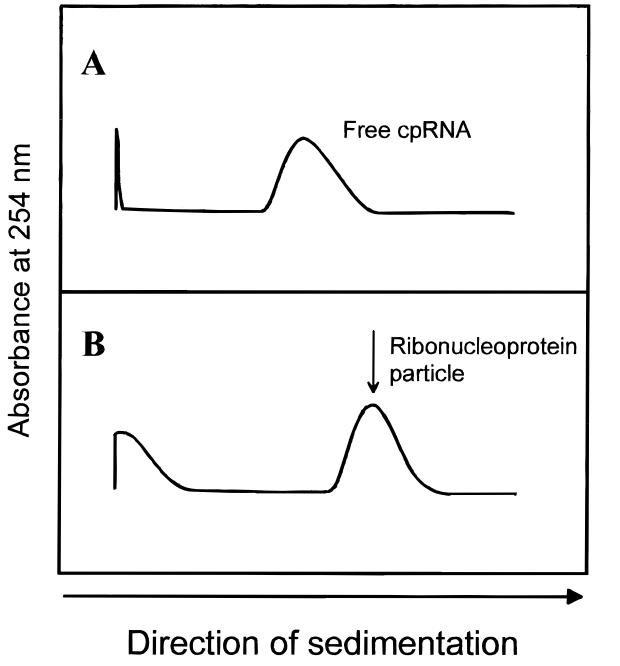

FIGURE 3. Sucrose gradient analysis of cp1337 (**A**) and of the ribonucleoprotein particle reconstituted when cp1337 was incubated with a threefold molar excess of ribosomal proteins (**B**). Centrifugation was through a 5–20% sucrose gradient in reconstitution buffer. The arrow points to the position of migration of the control particle formed by the association of the native 3′ major domain with ribosomal proteins, which coincides with that of the particle formed with cp1337. A similar profile was observed with all the cpRNAs investigated.

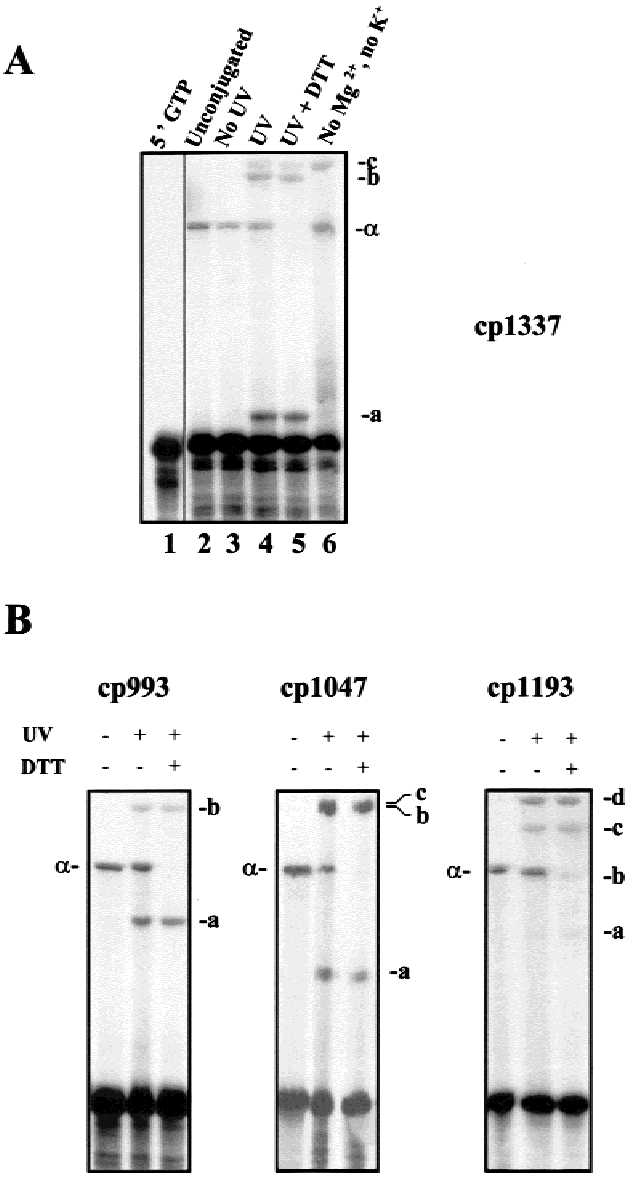

FIGURE 4. Identification of crosslinked species. **A:** Detailed analysis of intramolecular crosslinking of cp1337. Radiolabeled 5′-APA-cp1337 RNA (about 4 nM) was crosslinked under reconstitution conditions: 70 mM HEPES-KOH, pH 7.8, 20 mM $MgCl_2$, and 300 mM KCl or, when indicated, in the absence of Mg^{2+} and K^+. Crosslinked species and noncrosslinked RNA were resolved on denaturing 4% polyacrylamide gels. DTT was added to a final concentration of 1 mM prior to electrophoresis, when indicated. RNA was exposed to 310-nm UV light for 15 min, except in the No UV lane. The Unconjugated sample was not modified with APA and the 5′-GTP sample was generated by transcription in the absence of GMPS. Crosslinked species are identified with letters (a–d). Band α corresponds to a dimer where two 5′-GMPS-RNAs are linked by a disulfide bridge. **B:** Examples of analysis with 5′-APA-cp993, -cp1047 and -cp1193. Radiolabeled 5′-APA-cpRNAs were irradiated (+) or not (–) with 310-nm UV light. DTT was added to a final concentration of 1 mM prior to electrophoresis, when indicated.

the lower half of helix 34 (crosslink II), and also crosslinked to G993, in an adjacent position (crosslink III). Finally, G1337, in an internal loop located at the junction of helices 29, 30, 41, and 42 in the lower part of the domain, crosslinked to a single-stranded segment connecting helices 28 and 29 (crosslink VII) and to the central portion of helix 30 (crosslink VIII).

The length of the crosslinked regions is comparable to that observed by Pace and coworkers with RNase P RNA analyzed with the same approach (Chen et al., 1998), except in crosslinks I and II. In these crosslinks, G993 and G1047, respectively, crosslinked to an extensive region in one strand of the lower stem of helix 34. One could suggest that G993, being located in an internal loop, has greater flexibility than a 5′ terminus located in a helix, which could increase the size of the target hit by the crosslinking reagent. However, G1047, which is in a helix, also crosslinks to a large region. Moreover, the size of the regions to which G1337 crosslinks in crosslinks VII and VIII is less extensive than that of crosslinks I and II, although G1337 is located in an internal loop. Recent X-ray crystallographic and NMR studies with a variety of RNA molecules have shown that internal and hairpin loops can be highly structured in the presence of divalent cations (reviewed by Doudna & Cate, 1997; Ramos et al., 1997). We suggest that in reconstitution buffer the 5′ terminus of cpRNAs can be constrained as well, whether it is located in an internal loop or in a helix, and we hypothesize that the large size of the regions to which G993

TABLE 2. Analysis of crosslinked species.

Crosslinked species	Dependence on Mg^{2+} and K^+ [a]	Efficiency[b]	Crosslinked nucleotides	Crosslink number
native				
native a	−	7.0	Circular form[c]	
cp993				
993 a	+	7.0	G1190-A1191;U1205-G1206; C1209-G1215	I
993 b	−	2.4	Circular form[c]	
cp1047				
1047 a	−	8.4	U1205-C1214	II
1047 b	+	7.2	G993	III
1047 c	−	7.2	Circular form[c]	III
cp1193				
1193 a	+	0.9	1395 region[d]	IV
1193 b	+	1.6	C995-A996	V
1193 c	−	3.9	U1060-C1063	VI
1193 d	−	5.4	Circular form[c]	
cp1309				
1309 a	−	5.7	Circular form[c]	
cp1337				
1337 a	+	10.2	C934-A938	VII
1337 b	+	4.7	A1229-G1233	VIII
1337 c	−	2.1	Circular form[c]	
cp1343				
1343 a	−	3.9	Circular form[c]	
cp1353				
1353 a	−	6.2	Circular form[c]	

[a] − indicates that the crosslinked species is detected independently of the presence of Mg^{2+} and K^+, and + indicates that the crosslinked species disappears in the absence of Mg^{2+} and K^+.
[b] Efficiency indicates percent conversion to crosslinked species.
[c] Intramolecular crosslink between the 5′ and 3′ ends.
[d] The position of this crosslink could not be identified by primer extension and was assessed from the size of the lariat (see Fig. 6).

and G1047 crosslink reflects some unusual flexibility in the lower stem of helix 34.

DISCUSSION

We have undertaken a study of the conformation of the 3′ major domain of 16S rRNA, in the absence of proteins, using a site-directed crosslinking method. The crosslinks were generated in a high-ionic strength buffer, where this domain adopts a conformation recognized by the ribosomal proteins. The importance of rRNA warrants a detailed investigation of its higher-order structure. rRNA may have functioned at a time without the aid of proteins (Noller, 1993), and a large body of evidence supports the direct role of rRNA in protein synthesis (Green & Noller, 1997). A report by Nitta et al. (1998a,b) recently suggested that in vitro-transcribed naked 23S rRNA could have peptidyl transferase activity. Previously, Purohit & Stern (1994) had shown that a fragment of 16S rRNA corresponding to the decoding center of 16S rRNA had the capacity to interact with mRNA, tRNA anticodon stem-loop, and aminoglycoside antibiotics such as neomycin in a similar way as 16S rRNA within 30S subunit, indicating that this fragment is able to perform some of the functions of the ribosome.

Several of the crosslinks we observed in the free 3′ major domain are in agreement with proximity relationships that have been observed within the 30S subunit. Crosslink I, which joins position 993 to a segment encompassing nt 1205–1215, is consistent with a previous UV crosslink joining positions 991–1212. This crosslink was identified in 16S rRNA within the 30S subunit first by Stiege et al. (1988) and, later on, with a higher resolution, by Wilms et al. (1997). Also, crosslink IV, which links the upper stem of helix 34 to helix 28 in the free domain, agrees with a proximity relationship demonstrated between positions 1196 and 1395 in 16S rRNA within the 30S subunit, using crosslinking with mRNA analogs (Rinke-Appel et al., 1993; Juzumiene et al., 1995; Sergiev et al., 1997) or cleavage with mRNA modified with phenanthroline (Bucklin et al., 1997).

Crosslinks VII and VIII also indicate interesting tertiary interactions showing that position 1337 is linked

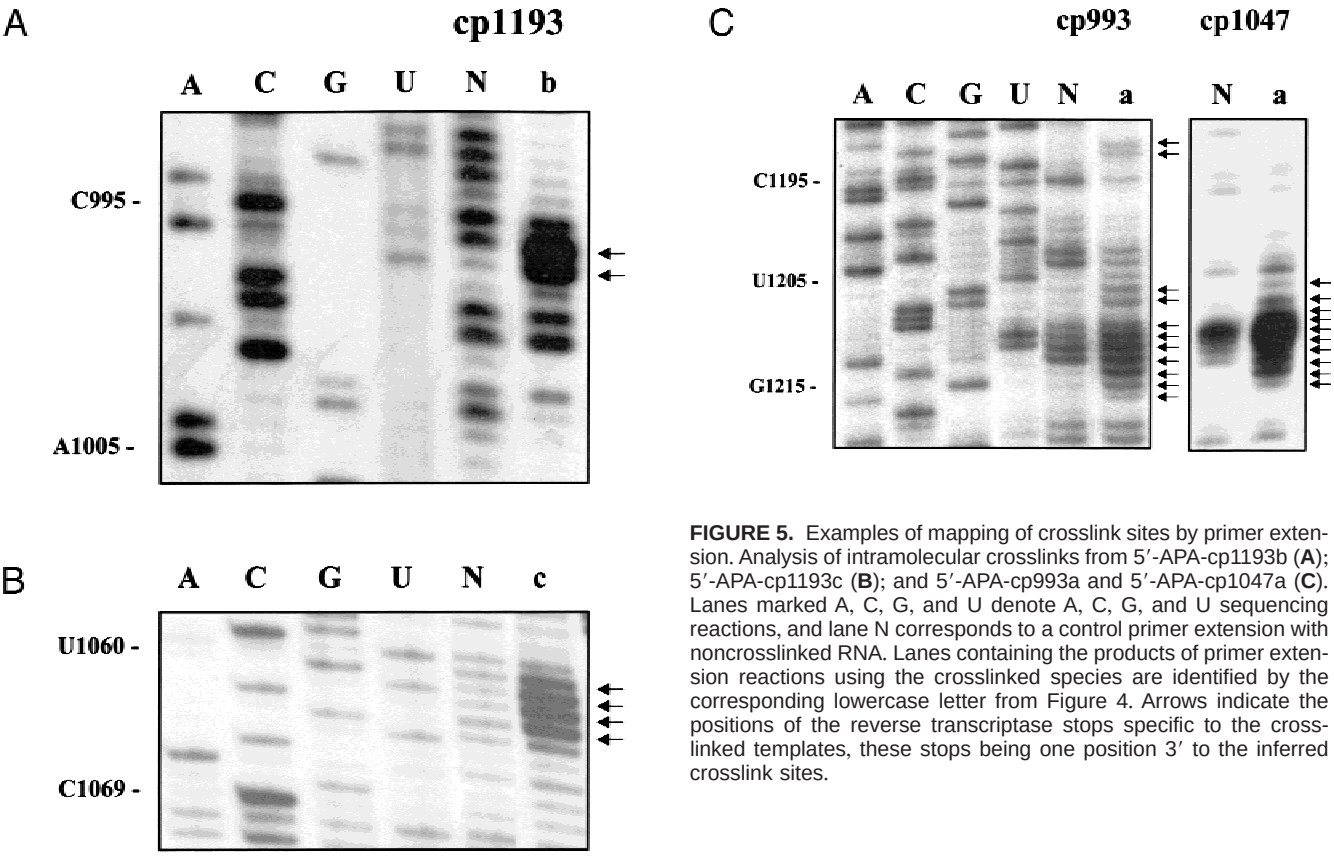

FIGURE 5. Examples of mapping of crosslink sites by primer extension. Analysis of intramolecular crosslinks from 5′-APA-cp1193b (**A**); 5′-APA-cp1193c (**B**); and 5′-APA-cp993a and 5′-APA-cp1047a (**C**). Lanes marked A, C, G, and U denote A, C, G, and U sequencing reactions, and lane N corresponds to a control primer extension with noncrosslinked RNA. Lanes containing the products of primer extension reactions using the crosslinked species are identified by the corresponding lowercase letter from Figure 4. Arrows indicate the positions of the reverse transcriptase stops specific to the crosslinked templates, these stops being one position 3′ to the inferred crosslink sites.

to nt 934–938, a segment connecting helices 28 to 29, and also to nt 1229–1233 in helix 30. The neighboring nucleotide G1338 is required for tRNA binding at the P site (von Ahsen & Noller, 1995) and has been crosslinked to the anticodon loop of P-site-bound tRNA, while position 936 has been crosslinked to the anticodon loop of tRNA bound at the A site (Döring et al., 1994). The obvious proximity between the anticodon loops of A-site- and P-site-bound tRNAs is in complete agreement with crosslink VII. As to crosslink VIII, which links position 1337 to the 1230 region, Noller and his coworkers also observed that these regions are proximal by probing 16S rRNA within the 30S subunit with hydroxyl radicals generated either with a tRNA anticodon stem-loop analog bound to the P site or with elongation factor G (Joseph et al., 1997; Wilson & Noller, 1998).

On the whole, our results strongly suggest that, when in solution in reconstitution buffer, the free RNA domain adopts a conformation that is similar to that within the 30S subunit. Nevertheless, this conformation probably differs in details from that within the 30S subunit. Ribosomal proteins have been shown to cause several local adjustments in the conformation of 16S rRNA, and they appear to stabilize rRNA tertiary structure and

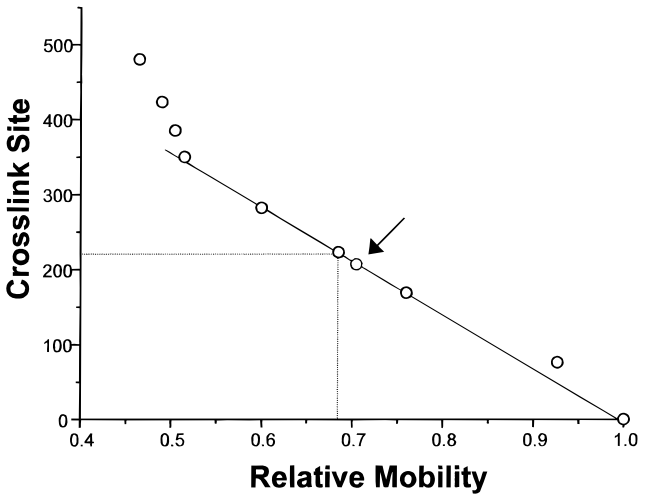

FIGURE 6. Correlation of crosslink site and mobility of crosslinked RNAs in denaturing polyacrylamide gels. The distance of crosslinked nucleotides to the 5′ terminus was plotted versus the crosslinked species mobility. This mobility is expressed relative to the mobility of the linear molecules, from the well to their final position (which was ascribed a value of 1). As an example, the relationship between the crosslink site and the relative mobility is indicated for band cp993a. The arrow points to the position of band cp1193a, for which the localization of the crosslink site could not be detected by primer extension but was inferred from its mobility.

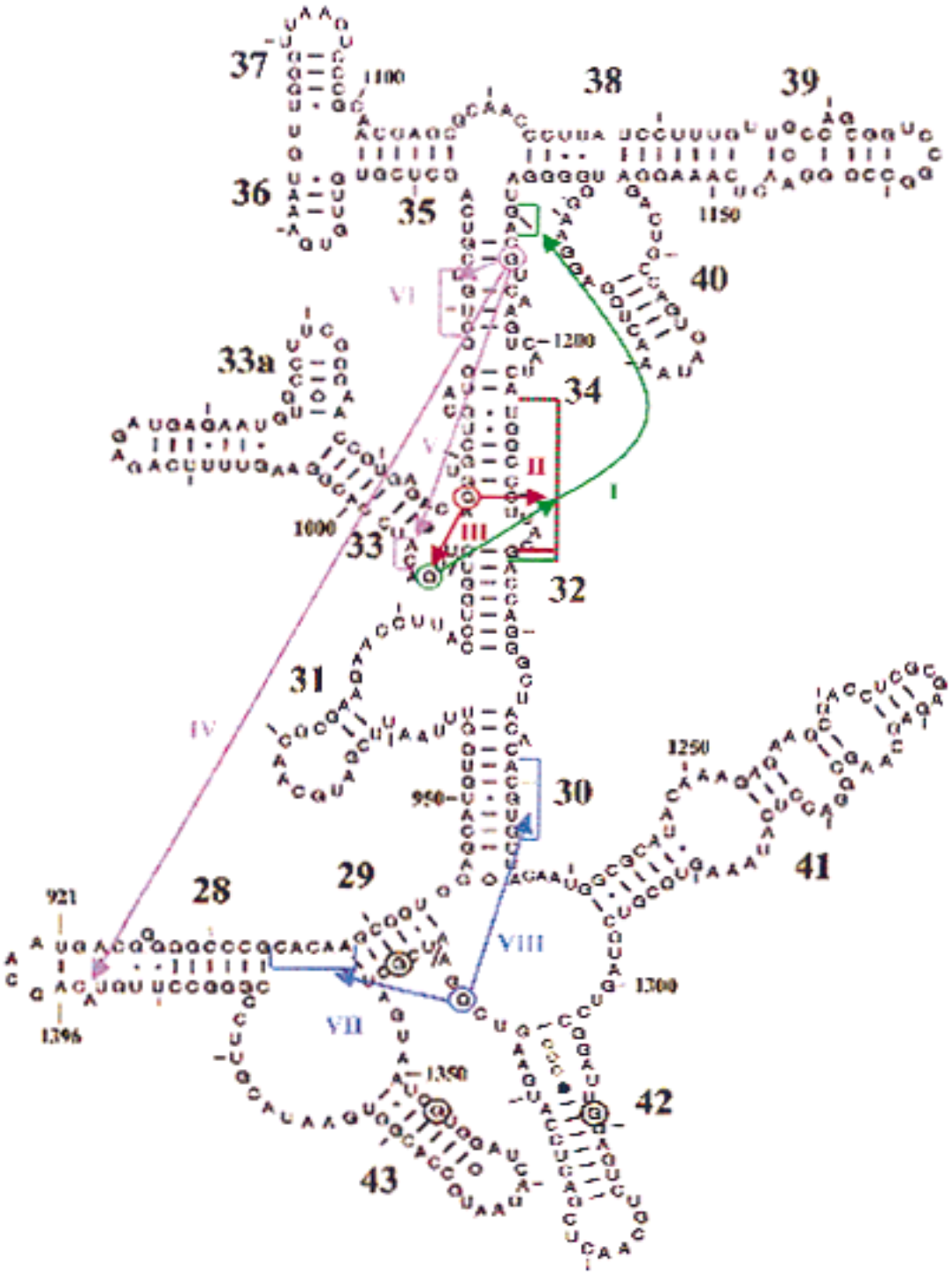

FIGURE 7. Overview of crosslinking results. Crosslinking results are shown in the secondary structure of the 3′ major domain, where arrows connect photoagent attachment sites (circles) to crosslink sites and are identified by roman numerals (see also Table 2).

facilitate conformational transitions (Baudin et al., 1989; Stern et al., 1989; see also Xing & Draper, 1995). However, the effect of ribosomal proteins on the conformation of rRNA was generally assessed in the nonphysiological high-ionic-strength reconstitution buffer. A careful study by Orr et al. (1998) recently demonstrated that an rRNA fragment containing the binding site for ribosomal protein S15 undergoes a significant and similar conformational change upon addition of either Mg^{2+} or protein S15, altering the orientation of a three-helical junction. It would be interesting to investigate with our crosslinking approach the conformation of the 3′ major

domain in a more physiological buffer than reconstitution buffer, in the absence or the presence of ribosomal proteins. This could help to better define the effect of ribosomal proteins on the conformation of rRNA.

We have obtained different crosslinks in helix 34 that suggest that the upper and lower portions of this important helix are in close proximity. Wilms et al. (1997) also concluded that this helix displays a bend, based on UV crosslinks in 16S rRNA within the 30S subunit. Although most of our crosslinks can readily be integrated in the current models depicting the folding of 16S rRNA within the 30S subunit (Mueller & Brimacombe, 1997a,b; Noller, 1998), we predict that helix 34 has a folded structure, in contrast with those models where it is extended. One logical interpretation is that helix 34 exists under different conformations and that we have identified one of these conformations. This is in agreement with various observations suggesting that helix 34 is highly flexible (see Laughrea & Tam, 1992; Brink et al., 1994; Mueller et al., 1997). Interestingly, a computational model by Fink et al. (1996) also considered the possibility that helix 34 is bent.

In conclusion, our results show that the site-directed crosslinking approach with cpRNAs can be applied to a large domain of 16S rRNA and generate valuable information that is consistent with existing results. Probing a large number of sites in this domain may contribute to refinement of its higher-order structure, a prerequisite to a detailed understanding of its function.

MATERIALS AND METHODS

Chemicals and enzymes

Except when noted, reagents were obtained commercially and used without further purification. *Deep Vent* DNA polymerase and PCR buffer were obtained from NEB; guanosine mono-phosphorothioate (GMPS) from USB; radiochemicals from ICN; RNA Guard, AMV reverse transcriptase, and restriction endonucleases from Pharmacia; and APA bromide and inorganic pyrophosphatase from Sigma.

Construction of pFD33

Plasmid pFD3 (Dragon & Brakier-Gingras, 1993) contains the sequence coding for the 3′ major and 3′ minor domains of *E. coli* 16S rRNA (nt 926–1542) under control of a T7 promoter. This plasmid was digested either with *Nde* I and *Apa* I to excise the T7 promoter, generating fragment 1, or with *Nde* I and *Rsa* I, generating fragment 2, which contains the T7 promoter and the region coding for the 3′ major domain. Fragments 1 and 2 were then ligated together, using a third fragment, a synthetic linker with a blunt end on one side and a cohesive *Apa* I end on the other side (resulting from the annealing of two oligonucleotides: 5′-ACAGCAATGAC GGGGGCC-3′ and 5′-CCCGTCATTGCTGT-3′). This three-fragment ligation generated pFD33, which contains two copies of the sequence coding for the 3′ major domain, one coding for nt 926–1396 and the other for nt 921–1393 of 16S rRNA, separated by a four-nucleotide sequence (see Fig. 1). In the cpRNAs, this sequence forms a tetraloop closing helix 28.

Preparation of cpRNAs

Template DNAs for in vitro transcription were synthesized by PCR from the tandemly repeated 3′ major domain genes of pFD33. Two primers were used to define the 5′ and 3′ termini of the RNAs that were produced (Table 1). The forward primers contained the promoter for T7 RNA polymerase. PCR reactions (100 μL) were performed using *Deep Vent* DNA polymerase in the commercial *Deep Vent* PCR buffer or in a 10-mM Tris-HCl buffer, at pH 8.3, containing 200 μM of each NTP, 50 mM KCl, 2.5 mM $MgCl_2$, 0.01% NP-40, 0.01% Triton X-100, 0.01 mg/mL bovine serum albumin, 10 ng template DNA and 25 pmol of the forward and the reverse primers. The amplification program was 25 cycles at 94 °C for 1 min, 45–57 °C for $1\frac{1}{2}$ min, depending on the primers used, and 72 °C for 1 min, followed by 5 min at 72 °C. The PCR products were subjected to gel electrophoresis on 1% agarose and purified from the gel with the GFX PCR kit (Pharmacia). The sequence of all cpRNA templates was verified by dideoxy-terminated sequencing (Sanger et al., 1977).

The native 3′ major domain (nt 926–1393) was produced by run-off transcription of the *Rsa* I product of pFD33 (Milligan & Uhlenbeck, 1989), using T7 RNA polymerase prepared by the method of Zawadzki & Gross (1991). The cpRNAs were produced by run-off transcription of the PCR templates. Preparative reactions (100 μL) contained 20 nM template, 80 mM HEPES-KOH, pH 7.5, 40 mM DTT, 12 mM $MgCl_2$, 2 mM spermidine, 2.5 mM of each NTP, 15 units of RNA Guard and 1.8 unit of inorganic pyrophosphatase. For the synthesis of RNAs containing GMPS at the 5′ end, the GTP concentration was reduced to 0.5 mM, the $MgCl_2$ concentration was raised to 22 mM and GMPS was added at a concentration of 6 mM. In analytical reactions, radiolabeled RNAs were produced in a 12.5 μL volume containing 25 μCi of [α-^{32}P]GTP (3,000 Ci/mmol) and 0.4 mM GTP in addition to the buffers and reagents mentioned above. Transcribed cpRNAs were gel-purified by electrophoresis through 4% polyacrylamide/8 M urea gels. RNAs were visualized by UV shadow or autoradiography, eluted in a 10 mM Tris-HCl buffer, at pH 8.0, containing 500 mM ammonium acetate, 1 mM EDTA, and 0.1% SDS, and precipitated with ethanol.

Reconstitution of cpRNAs into a ribonucleoprotein particle

The reconstitution of ribonucleoprotein particles was adapted from a standard method (Melançon et al., 1987). The 30S ribosomal proteins were isolated from 30S subunits of *E. coli* K12A19 by the LiCl–urea extraction procedure of Traub et al. (1971). Proteins and RNA were renatured separately. cpRNAs (about 120 μg) were preincubated at 43 °C for 30 min in reconstitution buffer (70 mM HEPES-KOH, pH 7.8, 300 mM KCl, 20 mM $MgCl_2$ and 6 mM β-mercaptoethanol). A threefold molar excess of 30S ribosomal proteins, also preincubated at 43 °C for 30 min in the same buffer, was then added to a final reaction volume of 3 mL. The mixture was incubated for 1 h at 43 °C and chilled on ice. The ribonucleoprotein particles

were analyzed on a 5–20% sucrose gradient (26,000 rpm, 22 h, SW28 rotor).

Crosslinking procedure and mapping of crosslink sites

Crosslinking experiments were performed essentially as described by Burgin & Pace (1990). APA bromide was conjugated to the unique sulfur at the 5′-terminal phosphate of GMPS RNA. Analytical reactions were carried out to detect the crosslinked species and to assess the efficiency of the crosslinks. In an analytical crosslinking reaction (100 μL), radiolabeled 5′-APA-RNA (about 4 nM) was incubated in reconstitution buffer without β-mercaptoethanol for 30 min at 43 °C and then chilled on ice for 5 min. The solution was exposed for 15 min at 4 °C to 310-nm UV light (Foto/PrepI, Fotodyne) at a distance of 5 cm. It was screened by a polystyrene filter (Petri dish, Fisher) to absorb wavelengths under 300 nm. In control experiments, the crosslinking reactions were performed in the absence of Mg^{2+} and K^{+} ions. The crosslinked species were resolved on 4% polyacrylamide/8 M urea gels, visualized by autoradiography, and the efficiency of the crosslinks was evaluated by measuring the intensity of the bands in percent of the total input, using Alpha Imager software (Alpha Innotech Corp.). The migration of the crosslinked species was assessed in the denaturing gel relative to the linear molecules. Preparative crosslinking reactions were carried out to isolate crosslinked species. In a preparative crosslinking reaction (100 μL), 5′-APA-RNA (at about 400 nM) was incubated as described for the analytical reactions. The crosslinked species, as well as the noncrosslinked RNA, were resolved by electrophoresis through 4% polyacrylamide/8 M urea gels, visualized by staining with ethidium bromide, eluted from the gel as described above, and used to map the crosslink sites by primer extension. Primers used were the reverse primers complementary to 16S rRNA described in Table 1. They were 5′-end-labeled with [γ-^{32}P]ATP (3,000 Ci/mmol) and annealed to crosslinked or noncrosslinked RNA in a 50 mM Tris-HCl buffer at pH 8.5 containing 100 mM KCl by heating for 2 min at 85 °C, followed by slow cooling to room temperature. The oligonucleotides were then extended with AMV reverse transcriptase. The products of extension were resolved by electrophoresis on 8% polyacrylamide/8 M urea gels.

ACKNOWLEDGMENTS

We thank Drs. L. DesGroseillers, F. Dragon, S. Michnick, and M. O'Connor for stimulating comments and critical reading of this manuscript. We also thank F. Bélanger for his contribution to some crosslinking experiments. This study was supported by a grant of the Medical Research Council of Canada to L.B.-G. A.M. held a studentship from the National Sciences and Engineering Research Council of Canada.

Received June 22, 1998; returned for revision July 24, 1998; revised manuscript received August 11, 1998

REFERENCES

Agalarov SC, Zheleznyakova EN, Selivanova OM, Zheleznaya LA, Matvienko NI, Vasiliev VD, Spirin AS. 1998. In vitro assembly of a ribonucleoprotein particle corresponding to the platform domain of the 30S ribosomal subunit. *Proc Natl Acad Sci USA 95*:999–1003.

Alexander RW, Cooperman BS. 1998. Ribosomal proteins neighboring 23S rRNA nucleotides 803–811 within the 50S subunit. *Biochemistry 37*:1714–1721.

Arkov AL, Freistroffer DV, Ehrenberg M, Murgola EJ. 1998. Mutations in RNAs of both ribosomal subunits cause defects in translation. *EMBO J 17*:1507–1514.

Ban N, Freeborn B, Nissen P, Penczek P, Grassucci RA, Sweet R, Frank J, Moore PB, Steitz TA. 1998. A 9 Å resolution X-ray crystallographic map of the large ribosomal subunit. *Cell 93*:1105–1115.

Baranov PV, Gurvich OL, Bogdanov AA, Brimacombe R, Dontsova OA. 1998a. New features of 23S ribosomal RNA folding: The long helix 41–42 makes a "U-turn" inside the ribosome. *RNA 4*:658–668.

Baranov PV, Sergiev PV, Dontsova OA, Bogdanov AA, Brimacombe R. 1998b. The database of ribosomal cross-links (DRC). *Nucleic Acids Res 26*:187–189.

Baudin F, Mougel M, Romby P, Eyermann F, Ebel JP, Ehresmann B, Ehresmann C. 1989. Probing the phosphates of the *Escherichia coli* ribosomal 16S RNA in its naked form, in the 30S subunit, and in the 70S ribosome. *Biochemistry 28*:5847–5855.

Bilgin N, Richter AA, Ehrenberg M, Dahlberg AE, Kurland CG. 1990. Ribosomal RNA and protein mutants resistant to spectinomycin. *EMBO J 9*:735–739.

Brimacombe R. 1991. RNA-protein interactions in the *Escherichia coli* ribosome. *Biochimie 73*:927–936.

Brink MF, Brink G, Verbeet MP, de Boer H. 1994. Spectinomycin interacts specifically with the residues G_{1064} and C_{1192} in 16S rRNA, thereby potentially freezing this molecule into an inactive conformation. *Nucleic Acids Res 22*:325–331.

Bucklin DJ, Vanwaes MA, Bullard JM, Hill WE. 1997. Cleavage of 16S rRNA within the ribosome by mRNA modified in the A-site codon with phenantroline-Cu(II). *Biochemistry 36*:7951–7957.

Burgin AB, Pace NR. 1990. Mapping the active site of ribonuclease P RNA using a substrate containing a photoaffinity agent. *EMBO J 9*:4111–4118.

Cate JH, Gooding AR, Podell E, Zhou K, Golden BL, Kundrot CE, Cech TR, Doudna JA. 1996. Crystal structure of a group I intron ribozyme domain: Principles of RNA packing. *Science 273*:1678–1685.

Chen JL, Nolan JM, Harris ME, Pace NR. 1998. Comparative photocrosslinking analysis of the tertiary structure of *Escherichia coli* and *Bacillus subtilis* RNase P RNAs. *EMBO J 17*:1515–1525.

Correll CC, Freeborn B, Moore PB, Steitz TA. 1997. Metals, motifs, and recognition in the crystal structure of a 5S rRNA domain. *Cell 91*:705–712.

Dallas A, Moore PB. 1997. The loop E–loop D region of *Escherichia coli* 5S RNA: The solution structure reveals an unusual loop that may be important for binding ribosomal proteins. *Structure 5*:1639–1653.

Döring T, Mitchell P, Osswald M, Bochkariov D, Brimacombe R. 1994. The decoding region of 16S RNA; a cross-linking study of the ribosomal A, P and E sites using tRNA derivatized at position 32 in the anticodon loop. *EMBO J 13*:2677–2685.

Doudna JA, Cate JH. 1997. RNA structure: Crystal clear? *Curr Opin Struct Biol 7*:310–316.

Dragon F, Brakier-Gingras L. 1993. Interaction of *Escherichia coli* ribosomal protein S7 with 16S rRNA. *Nucleic Acids Res 21*:1199–1203.

Fink DL, Chen RO, Noller HF, Altman RB. 1996. Computational methods for defining the allowed conformational space of 16S rRNA based on chemical footprinting data. *RNA 2*:851–866.

Fourmy D, Recht MI, Blanchard SC, Puglisi JD. 1996. Structure of the A site of *Escherichia coli* 16S ribosomal RNA complexed with an aminoglycoside antibiotic. *Science 274*:1367–1371.

Green R, Noller HF. 1997. Ribosomes and translation. *Annu Rev Biochem 66*:679–716.

Harris ME, Kazantsev AV, Chen JL, Pace NR. 1997. Analysis of the tertiary structure of the ribonuclease P ribozyme-substrate complex by site-specific photoaffinity crosslinking. *RNA 3*:561–576.

Harris ME, Nolan JM, Malhotra A, Brown JW, Harvey SC, Pace NR. 1994. Use of photoaffinity crosslinking and molecular modeling to

analyse the global architecture of ribonuclease P RNA. *EMBO J 13*:3953–3963.
Herr W, Chapman NM, Noller HF. 1979. Mechanism of ribosomal subunit association: Discrimination of specific sites in 16S RNA essential for association activity. *J Mol Biol 130*:433–449.
Joseph S, Weiser B, Noller HF. 1997. Mapping the inside of the ribosome with an RNA helical ruler. *Science 278*:1093–1098.
Juzumiene DI, Shapkina TG, Wollenzien P. 1995. Distribution of cross-links between mRNA analogues and 16S rRNA in *Escherichia coli* 70S ribosomes made under equilibrium conditions and their response to tRNA binding. *J Biol Chem 270*:12794–12800.
Laughrea M, Tam J. 1992. In vivo chemical footprinting of the *Escherichia coli* ribosome. *Biochemistry 31*:12035–12041.
Makosky PC, Dahlberg AE. 1987. Spectinomycin resistance at site 1192 in 16S ribosomal RNA of *E. coli*: An analysis of three mutants. *Biochimie 69*:885–889.
Melançon P, Gravel M, Boileau G, Brakier-Gingras L. 1987. Reassembly of active 30S ribosomal subunits with unmethylated in vitro transcribed 16S rRNA. *Biochem Cell Biol 65*:1022–1030.
Milligan JF, Uhlenbeck OC. 1989. Synthesis of small RNAs using T7 RNA polymerase. *Methods Enzymol 180*:51–62.
Moazed D, Noller HF. 1990. Binding of tRNA to the ribosomal A and P sites protects two distinct sets of nucleotides in 16S rRNA. *J Mol Biol 211*:135–145.
Moine H, Dahlberg AE. 1994. Mutations in helix 34 of *Escherichia coli* 16 S ribosomal RNA have multiple effects on ribosome function and synthesis. *J Mol Biol 243*:402–412.
Mueller F, Brimacombe R. 1997a. A new model for the three-dimensional folding of *Escherichia coli* 16S ribosomal RNA. I. Fitting the RNA to a 3D electron microscopic map at 20 Å. *J Mol Biol 271*:524–544.
Mueller F, Brimacombe R. 1997b. A new model for the three-dimensional folding of *Escherichia coli* 16S ribosomal RNA. II. The RNA-protein interaction data. *J Mol Biol 271*:545–565.
Mueller F, Stark H, van Heel M, Rinke-Appel J, Brimacombe R. 1997. A new model for the three-dimensional folding of *Escherichia coli* 16S ribosomal RNA. III. The topography of the functional centre. *J Mol Biol 271*:566–587.
Murgola EJ. 1996. Ribosomal RNA in peptide chain termination. In: Zimmermann RA, Dahlberg AE, eds. *Ribosomal RNA: Structure, evolution, processing and function in protein biosynthesis*. New York/London: CRC Press. pp 357–369.
Nitta I, Kamada Y, Noda H, Ueda T, Watanabe K. 1998a. Reconstitution of peptide bond formation with *Escherichia coli* 23S ribosomal RNA domains. *Science 281*:666–669.
Nitta I, Ueda T, Watanabe K. 1998b. Possible involvement of *Escherichia coli* 23S ribosomal RNA in peptide bond formation. *RNA 4*:257–267.
Nolan JM, Burke DH, Pace NR 1993. Circularly permuted tRNAs as specific photoaffinity probes of ribonuclease P RNA structure. *Science 261*:762–765.
Noller HF. 1993. On the origin of the ribosome: Coevolution of subdomain of tRNA and rRNA. In: Gesteland RF, Atkins JF, eds. *The RNA World*. Cold Spring Harbor, New York: Cold Spring Harbor Laboratory Press. pp 137–156.
Noller HF. 1998. Ribosomal RNA. In: Simons RW, Grunberg-Manago M, eds. *RNA Structure and function*. Cold Spring Harbor, New York: Cold Spring Harbor Laboratory Press. pp 253–278.
O'Connor M, Thomas CL, Zimmermann RA, Dahlberg AE. 1997. Decoding fidelity at the ribosomal A and P sites: Influence of mutations in three different regions of the decoding domain in 16S rRNA. *Nucleic Acids Res 25*:1185–1193.
Oehler R, Polacek N, Steiner G, Barta A. 1997. Interaction of tetracycline with RNA–photoincorporation into ribosomal RNA of *Escherichia coli*. *Nucleic Acids Res 25*:1219–1224.
Orr JW, Hagerman PJ, Williamson JR. 1998. Protein and Mg^{2+}-induced conformational changes in the S15 binding site of 16S ribosomal RNA. *J Mol Biol 275*:453–464.
Purohit P, Stern S. 1994. Interactions of a small RNA with antibiotic and RNA ligands of the 30S subunit. *Nature 370*:659–662.
Ramos A, Gubser CC, Varani G. 1997. Recent solution structures of RNA and its complexes with drugs, peptides and proteins. *Curr Opin Struct Biol 7*:317–323.
Rinke-Appel J, Jünke N, Brimacombe R, Lavrik I, Dokudovskaya S, Dontsova O, Bogdanov A. 1993. Site-directed cross-linking of mRNA analogues to 16S ribosomal RNA; a complete scan of cross-links from all positions between '+1' and '+16' on the mRNA, downstream from the decoding site. *Nucleic Acids Res 21*:2853–2859.
Samaha RR, O'Brien B, O'Brien TW, Noller HF. 1994. Independent in vitro assembly of a ribonucleoparticle containing the 3′ domain of 16S rRNA. *Proc Natl Acad Sci USA 91*:7884–7888.
Sanger F, Nicklen S, Coulson AR. 1977. DNA sequencing with chain-terminating inhibitors. *Proc Natl Acad Sci USA 74*:5463–5467.
Sergiev PV, Lavrik IN, Wlasoff VA, Dokudovskaya SS, Dontsova OA, Bogdanov AA, Brimacombe R. 1997. The path of mRNA through the bacterial ribosome: A site-directed crosslinking study using new photoreactive derivatives of guanosine and uridine. *RNA 3*:464–475.
Stiege W, Kosack M, Stade K, Brimacombe R. 1988. Intra-RNA cross-linking in *Escherichia coli* 30S ribosomal subunits: Selective isolation of cross-linked products by hybridization to specific cDNA fragments. *Nucleic Acids Res 16*:4315–4329.
Stern S, Powers T, Changchien LM, Noller HF. 1989. RNA-protein interactions in 30S ribosomal subunits: Folding and function of 16S rRNA. *Science 244*:783–790.
Szewczak AA, Moore PB. 1995. The sarcin ricin loop, a modular RNA. *J Mol Biol 247*:81–98.
Thygesen J, Weinstein S, Franceschi F, Yonath A. 1996. The suitability of multi-metal clusters for phasing in crystallography of large macromolecular assemblies. *Structure 4*:513–518.
Traub P, Mizushima S, Lowary CV, Nomura M. 1971. Reconstitution of ribosomes from subribosomal components. *Methods Enzymol 20*:391–407.
Viani-Puglisi E, Green R, Noller HF, Puglisi JD. 1997. Structure of a conserved RNA component of the peptidyl transferase centre. *Nature Struct Biol 4*:775–778.
von Ahsen U, Noller HF. 1995. Identification of bases in 16S rRNA essential for tRNA binding at the 30S ribosomal P site. *Science 267*:234–237.
Wakao H, Romby P, Ebel JP, Grunberg-Manago M, Ehresmann C, Ehresmann B. 1991. Topography of the *Escherichia coli* ribosomal 30S subunit-initiation factor 2 complex. *Biochimie 73*:991–1000.
Weitzmann CJ, Cunningham PR, Nurse K, Ofengand J. 1993. Chemical evidence for domain assembly of the *Escherichia coli* 30S ribosome. *FASEB J 7*:177–180.
Wilms C, Noah JW, Zhong D, Wollenzien P. 1997. Exact determination of UV-induced crosslinks in 16S ribosomal RNA in 30S ribosomal subunits. *RNA 3*:602–612.
Wilson KS, Noller HF. 1998. Mapping the position of translational elongation factor EF-G in the ribosome by directed hydroxyl radical probing. *Cell 92*:131–139.
Xing Y, Draper DE. 1995. Stabilization of a ribosomal RNA tertiary structure by ribosomal protein L11. *J Mol Biol 249*:319–331.
Zawadzki V, Gross HJ. 1991. Rapid and simple purification of T7 RNA polymerase. *Nucleic Acids Res 19*:1948.
Zimmermann RA. 1996. The decoding domain. In: Zimmermann RA, Dahlberg AE, eds. *Ribosomal RNA: Structure, evolution, processing and function in protein biosynthesis*. New York/London: CRC Press. pp 277–309.